Effect of substrate and orientation on charge ordering behaviors in epitaxial $Pr_{0.5}Ca_{0.35}Sr_{0.15}MnO_3$ films

H. W. Yang,[1] C. Wang,[2] R. S. Cai,[2] F. X. Hu,[1] Y. Q. Wang,[2,3,a)] and J. R. Sun[1,a)]
[1]*Beijing National Laboratory for Condensed Matter and Institute of Physics, Chinese Academy of Sciences, Beijing 100190, People's Republic of China*
[2]*The Cultivation Base for State Key Laboratory, Qingdao University, No. 308 Ningxia Road, Qingdao 266071, People's Republic of China*
[3]*College of Physics, Qingdao University, No. 308 Ningxia Road, Qingdao 266071, People's Republic of China*

(Presented 5 November 2014; received 5 September 2014; accepted 27 October 2014; published online 27 February 2015)

The charge ordering (CO) behaviors of $Pr_{0.5}Ca_{0.35}Sr_{0.15}MnO_3$ films grown on STO(100), STO(110) and LAO(100) are systematically investigated by transport measurements and transmission electron microscopy (TEM) examinations. From the transport measurements, the CO transition temperatures of all the three films are much higher than those of the bulk materials, showing that the film strain could enhance the CO transition. From TEM observations, many superlattice spots appear in the electron diffraction patterns taken from the films, indicating the appearance of the CO modulation structures at room temperature. The modulation vectors are determined to be (1/2, 0, 0) for STO (100), (1/2, 1/2, 1/2) for STO (110), and both (0, 1/2, 0) and (1/2, 1/2, 0) for LAO (100). It is shown that both the substrate orientation and the film strain have a great effect on the CO modulation structures. The CO state is much easier to appear in the compressive strain direction which is due to the Mn-O-Mn angle tilting. © *2015 AIP Publishing LLC*. [http://dx.doi.org/10.1063/1.4913731]

INTRODUCTION

Due to the strong correlation among the spin, charge, orbital and lattice, perovskite oxides exhibit many fascinating properties, such as colossal magnetoresistance and multiferroics. The charge and orbital order (CO-OO) as one of the characteristic phenomena in the perovskite manganite system has attracted much interest for its strong response to the magnetic field, electric field and pressure.[1,2] Using high resolution transmission electron microscopy (HRTEM), Uehara *et al.*[3] demonstrated that a phase separation took place in bulk $La_{5/8-y}Pr_yCa_{3/8}MnO_3$, a sub-micrometer-scale of CO insulating and FM metal domains. Tao *et al.*[4] also directly observed the existence of the CO nanoscale phase in bulk $La_{0.55}Ca_{0.45}MnO_3$ using low-temperature TEM. Asaka *et al.*[5] found that two types of superlattice spots appeared below 230 K and 150 K in bulk $Pr_{3/8}Ca_{5/8}MnO_3$, the first is caused by the formation of $d_{3x^2-r^2}/d_{3y^2-r^2}$ type of CO, and the second results from the order of excess $1/8Mn^{3+}$. However, for the epitaxial films the CO behaviors are quite different from those in the bulk due to the existence of strain in the epitaxial films.[6–10] Combined transport measurements with TEM examinations, Yang *et al.*[11] studied the effect of substrate and film thickness on the CO behaviors of $Pr_{0.5}Ca_{0.5}MnO_3$ films, and found that the CO transition temperature (T_{CO}) for the film on LAO(100) is lower while the T_{CO} for the film on STO(100) is higher than that of bulk $Pr_{0.5}Ca_{0.5}MnO_3$. Chen *et al.*[12,13] and Wang *et al.*[14–16] showed that the film thickness and substrate orientation have a great effect on the CO behaviors in $Bi_{0.4}Ca_{0.6}MnO_3$ and $Sm_{0.5}Ca_{0.5}MnO_3$ epitaxial films.

$Pr_{1-x}(Ca_{1-y}Sr_y)_xMnO_3$ has an orthorhombic structure with a space group of Pbnm ($a_0 = \sqrt{2}a_c, b_0 = \sqrt{2}a_c, c_0 = \sqrt{2}a_c$, where a_c is the lattice parameter of pseudocubic structure). It has a narrow e_g band and its physical properties vary greatly as the x or y changes.[17–22] Tomioka and Tokura[23] obtained the phase diagram and lattice parameters of $Pr_{1-x}(Ca_{1-y}Sr_y)_xMnO_3$ with different x and y, which may convert from CO state to ferromagnetic metal (FM) state. From the phase diagram it is demonstrated that the bulk $Pr_{0.5}Ca_{0.35}Sr_{0.15}MnO_3$ (PCSMO) is in CO state at low temperature and the T_{CO} is about 190 K. Zhao *et al.*[24] studied the effect of the substrate on the CO phase and transport behaviors, and showed that a large magnetic field is needed to melt CO phase if the film suffers tensile strain, indicating that tensile strain could enhance the stability of CO phase.

The CO behaviors are usually studied by temperature *vs.* resistance R(T) or temperature-dependence magnetization M(T). However, by R(T) or M(T), it is difficult to determine which direction is much easier for the CO modulation to appear, and the effect of film strain on the CO behaviors. In this paper, the 110-nm-thick PCSMO films on STO(100), STO(110), and LAO(100) were prepared and the effect of substrate strain and film orientation on the CO behaviors was systematically investigated by combining transport measurements with TEM.

EXPERIMENTAL

110-nm-thick PCSMO films were deposited on STO(100), STO(110), and LAO(100) substrates by the pulsed laser deposition at 720 °C with an oxygen pressure of 90 Pa. The laser

a)Authors to whom correspondence should be addressed. Electronic addresses: yqwang@qdu.edu.cn and jrsun@iphy.ac.cn

source is KrF excimer laser with $\lambda = 248$ nm and the repetition frequency of deposition is 1 Hz. The targets were prepared by a conventional solid-phase sintering of Pr_6O_{11}, $CaCO_3$, $SrCO_3$, and MnO_2 powders. Structural characterization of the sintering product was performed using X-ray diffraction (XRD) with Cu Kα radiation ($\lambda = 1.5406$ Å). The magnetic and transport measurements were performed with a Quantum Design superconducting quantum interference device magnetometer and a physical property measurement system, respectively. Specimens for TEM observations were prepared in a cross-sectional orientation using conventional mechanical polishing and ion thinning techniques. Selected-area electron diffraction (SAED) and HRTEM examinations were carried out using a JEOL JEM 2100F transmission electron microscope operating at 200 kV.

RESULTS AND DISCUSSION

Figure 1 is a typical XRD pattern of the PCSMO films. The sharp peaks indicate that the films have a good epitaxial relationship with the substrates of STO(100) (a = 3.905 Å) and LAO(100) (a = 3.79 Å). The epitaxial direction of the films is along [100] axis. For the STO(100) and LAO(100), the out-of-plane lattice parameters of the films are 3.76 Å and 3.88 Å, respectively, indicating that the films suffer in-plane tensile strain on STO(100) and compressive strain on LAO(100), compared to bulk PCSMO (a = 3.836 Å). Whereas for the STO(110) the film grows along [101] axis, the out-of-plane spacing of d_{101} is 2.68 Å showing that the film suffers in-plane tensile strain.

Fig. 2 shows the temperature dependence of zero-field cooling (ZFC) and field cooling (FC) magnetization and the resistance versus temperature curves for the bulk PCSMO, which are measured under 0.1 T. From Fig. 2(a), it exhibits paramagnetic at high temperature and possesses two transition points as the temperature decreases. The T_{CO} appears at about 220 K, which is higher than ~190 K reported in previous work.[23] For PCSMO films, it is quite difficult to recognize the T_{CO} from the M(T) measurements, so the R(T) curve is applied. The warming temperature dependence of resistance for PCSMO films on different substrates is

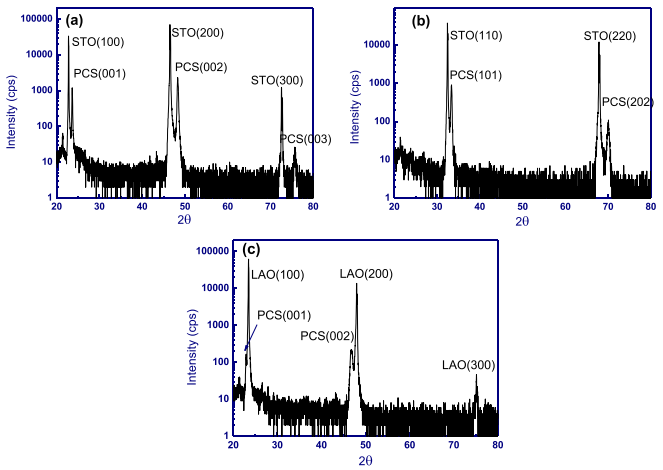

FIG. 1. XRD spectra of PCSMO films on the substrates (a) STO(100), (b) STO(110), and (c) LAO(100).

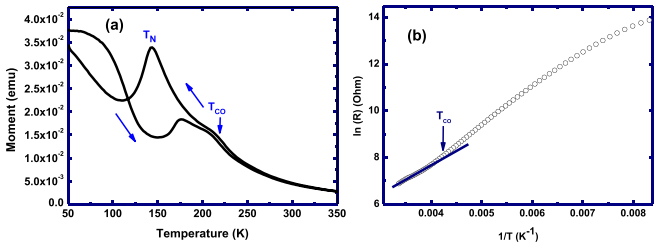

FIG. 2. The temperature dependence of magnetization ZFC and FC under 0.1 T (a) and the resistance plot of ln(R) versus 1/T (b) for bulk PCSMO.

measured and the curve of ln(R) versus 1/T is plotted in Fig. 3. The T_{CO} of the three films are all much higher than that of the bulk material. It is shown that the CO state is more stable in films than that in bulk materials indicating the strain could stabilize the CO state. The T_{CO} of film on STO(100) is higher than others, and the CO state is more stable. Therefore the substrate strain and orientation can affect the CO state.

To investigate the effect of substrate strain and film orientation on the CO behaviors, extensive SAED and HRTEM examinations at room temperature and 103 K were performed. Fig. 4(a) is the [001] zone-axis SAED pattern of PCSMO/STO(100) film recorded at room temperature. The epitaxial PCSMO film is along [100] direction which matches well with the STO(100). Except the normal diffraction spots, some superlattice spots appear in the SAED pattern, which are the characteristic of the CO phase in good agreement with the R(T) results. The spots only appear along the [100] axis, and no other direction of the superlattice spots is observed, so the CO phase only appears along [100] axis. The modulated periodicity is about two times of d_{100} spacing and the modulated vector is determined to be (1/2, 0, 0). Fig. 4(b) is the corresponding HRTEM image. Clear stripes along the [100] direction could be seen from the image, and no other direction of stripes appears consistent with the SAED results. The modulated periodicity is about 7.6 Å. The corresponding schematic model is proposed in Fig. 4(c). The modulation structure is two times of the d_{100} spacing,

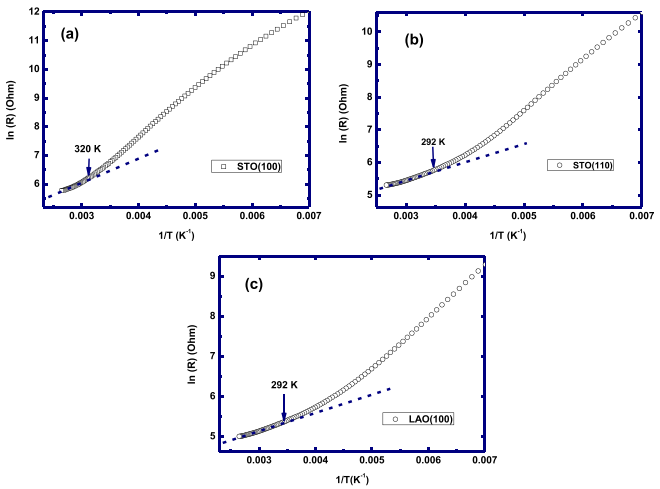

FIG. 3. The resistance plots of ln(R) versus 1/T for PCSMO films on STO(100), STO(110) and LAO(100). The black arrows present the T_{CO} and antiferromagnetic transition temperature (T_N).

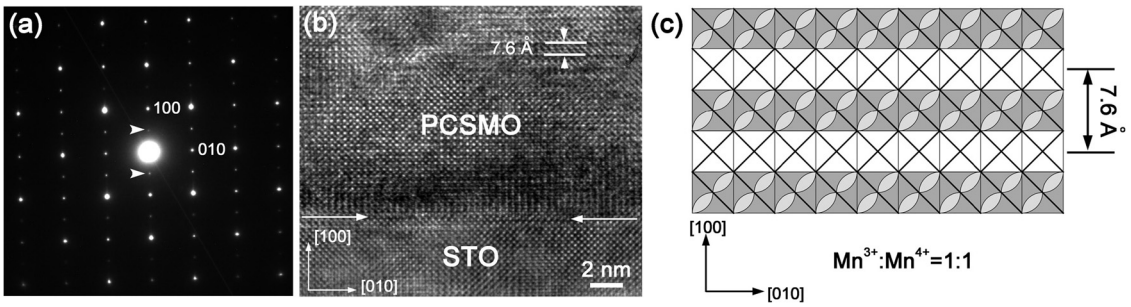

FIG. 4. The SAED pattern (a), HRTEM image (b), and schematic model (c) for PCSMO/STO(100) film, ⊠ and ⊠ represent Mn^{3+} and Mn^{4+}, respectively.

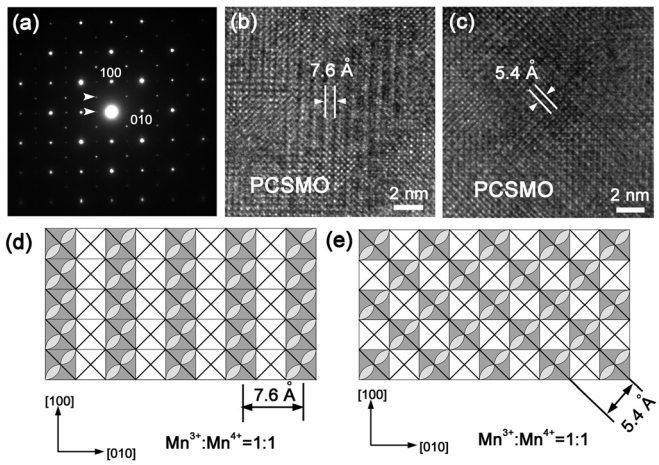

FIG. 5. The SAED pattern (a), HRTEM image (b), and schematic model (c) for PCSMO/LAO(100) film, ⊠ and ⊠ represent Mn^{3+} and Mn^{4+}, respectively.

and therefore the ratio of Mn^{3+} and Mn^{4+} should be 1:1 in the chemical composition, keeping electric neutrality of the crystal. The film suffers tensile strain in plane and compressive strain out of plane, and the modulation structure only appears in the compressive direction, indicating the CO phase is easier to emerge under compressive strain. When the temperature decreases to 103 K, no additional superlattice spots in diffraction patterns are found, and only the area with modulation stripe becomes larger. Though the tensile strain could stabilize the CO behavior, the direction of compressive strain is much easier to form the CO phase.

Fig. 5 exhibits the [001] zone-axis HRTEM image and SAED pattern of PCSMO/LAO(100) film recorded at room temperature. The epitaxial film is along [100] direction, the same as PCSMO/STO(100) film, whereas the superlattice spots are different. Two types of CO modulation spots appear in PCSMO/LAO(100) film, one being along [010] direction and the other being along [110] direction. The modulation periodicity is two times of d_{010} and d_{110} spacing, respectively. In [100] direction, no superlattice spots appear showing no CO phase emerges in the direction. From the HRTEM image, two types of the stripes could also be seen and the periodicity is 7.6 Å and 5.4 Å, respectively. The modulated vectors are (0, 1/2, 0) and (1/2, 1/2, 0). Two kinds of corresponding schematic models are proposed in Figs. 5(d) and 5(e), and the Mn^{3+} and Mn^{4+} are arranged in order with a ratio of 1:1 ensuring the neutral charge. In the [010] direction, the film suffers compressive strain and the modulation appears, whereas the film suffers tensile stain in [100] direction and no superlattice spots are observed. It is consistent with the results of the film on STO.

The effect of substrate orientation on the CO behaviors was also studied. The $[10\bar{1}]$ zone-axis SAED pattern and HRTEM image of PCSMO/STO(110) film are shown in Fig. 6. The epitaxial orientation of PCSMO/STO(110) film is along [101], and the superlattice spots appear along the [111] direction in the SAED pattern which is different from the film on STO(100). No other superlattice spots are observed in [101] and [010] directions. In the HRTEM image, the modulation stripe appears only in the [111] direction, and the periodicity is 4.4 Å, two times of the lattice spacing of d_{111}. From the schematic model, we can see the ratio of Mn^{3+} and Mn^{4+} is 1:1 in the chemical composition, and for every Mn^{3+}, the nearest neighbor is Mn^{4+}. The [111] should be easier than other axis to appear modulation structures. The substrate orientation can also affect the direction of CO behaviors.

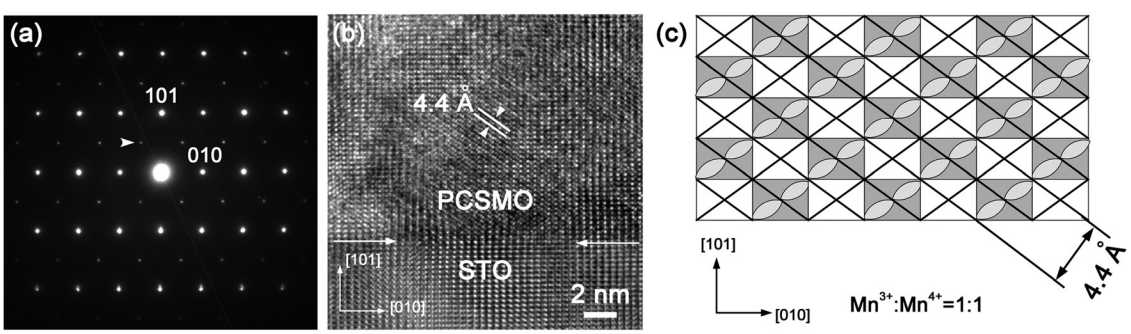

FIG. 6. The SAED pattern (a), HRTEM image (b), and schematic model (c) for PCSMO/STO(110) film, ⊠ and ⊠ represent Mn^{3+} and Mn^{4+}, respectively.

Though films on three substrates all appear CO state, the modulated direction is different, [100] on STO(100), [111] on STO(111), and both [110] and [010] on LAO(100). The CO state is greatly affected by the strain, which could be tuned by the substrates. The lattice mismatch σ is calculated by $\sigma = (a_s - a_f)/a_s$, where a_s is the lattice constant of the substrate and a_f is that of the film. It is 1.3%, 1.9%, and −1.0% for the film on three substrates, respectively. On STO, the film suffers tensile strain in plane, but compressive strain on LAO substrate. The Mn-O octahedron distortion in the films is very sensitive to the external strain. When suffered tensile strain, the distortion makes Mn-O bond elongated and Mn-O-Mn angle increased, and when suffered compressive strain, it is opposite.[25] The transition properties t_h of the electrons could be expressed by Mn-O-Mn bond length d and bond angle ϕ: $t_h \propto \cos\phi/d^{3.5}$.[26] From the formula, it is shown that Mn-O bond increase is beneficial to the appearance of the CO, while Mn-O-Mn angle increase is inverse, and therefore they compete with each other. On STO(100), CO state is along the compressive strain direction of [100], indicating that the Mn-O-Mn angle tilting is more important than bond length change. On STO(110), the strain release is different, and Mn-O bond length and Mn-O-Mn angle compete with each other, so CO state only appears in the [111] direction, which makes the system more stable. Whereas on LAO(100), CO state appears in both [010] and [110] direction, the former being similar to STO(100) for the angle tilting, and the latter being similar to STO(110) to make the structure more stable. That he T_{CO} of STO(100) is higher than LAO(100) should be due to the Mn-O-Mn angle tilting difference induced by the strain in the epitaxial film.

CONCLUSIONS

By transport measurements and TEM, the effects of substrate orientation and film strain on the CO behaviors of PCSMO films were investigated. From M(T) and R(T) curve, the T_{CO} of the films are much higher bulk PCSMO. The external strain can enhance CO phase. From TEM observations, the superlattice spots in the diffraction pattern and the HRTEM stripe images indicate the appearance of the CO modulated structures at room temperature. The modulation vectors are (0, 0, 1/2) for STO (100), (1/2, 1/2, 1/2) for STO (110), and (0, 1/2, 0) and (1/2, 1/2, 0) for LAO(100), showing that both the substrate orientation and film strain have a great effect on the CO phase direction. The CO state is much easier to appear in the compressive strain direction due to the Mn-O-Mn angle tilting.

ACKNOWLEDGMENTS

The authors would like to acknowledge the financial support from the National Natural Science Foundation of China (Grant No.: 10974105), and the Program of Science and Technology in Qingdao City (Grant No.: 11-2-4-23-hz). Y. Q. Wang would like to thank the financial support from the Top-notch Innovative Talent Program of Qingdao City (Grant No.: 13-CX-8), and Taishan Outstanding Overseas Scholar Program of Shandong Province.

[1]Y. Tokura and N. Nagaosa, Science **288**, 462 (2000).
[2]Y. Wakabayashi, D. Bizen, H. Nakao, Y. Murakami, M. Nakamura, Y. Ogimoto, K. Miyano, and H. Sawa, Phys. Rev. Lett. **96**, 017202 (2006).
[3]M. Uehara, S. Mori, C. H. Chen, and S. W. Cheong, Nature **399**, 560 (1999).
[4]J. Tao, D. Niebieskikwiat, M. Varela, W. Luo, M. A. Schofield, Y. Zhu, M. B. Salamon, J. M. Zuo, S. T. Pantelides, and S. J. Pennycook, Phys. Rev. Lett. **103**, 097202 (2009).
[5]T. Asaka, S. Yamada, S. Tsutsumi, C. Tsuruta, K. Kimoto, T. Arima, and Y. Matsui, Phys. Rev. Lett. **88**, 097201 (2002).
[6]E. Rauwel, W. Prellier, B. Mercey, S. de Brion, and G. Chouteau, J. Appl. Phys. **98**, 093903 (2005).
[7]W. Prellier, A. M. Haghiri-Gosnet, B. Mercey, P. Lecoeur, M. Hervieu, C. Simon, and B. Raveau, Appl. Phys. Lett. **77**, 1023 (2000).
[8]V. Agarwal, R. Prasad, M. P. Singh, P. K. Siwach, A. Srivastava, P. Fournier, and H. K. Singh, Appl. Phys. Lett. **96**, 052512 (2010).
[9]Y. Q. Zhang, Z. D. Zhang, and J. Aarts, Phys. Rev. B **79**, 224422 (2009).
[10]T. Zhang, Q. Wei, R. K. Zheng, X. P. Wang, and Q. F. Fang, J. Appl. Phys. **113**, 013705 (2013).
[11]Z. Q. Yang, Y. Q. Zhang, J. Aarts, M. Y. Wu, and H. W. Zandbergen, Appl. Phys. Lett. **88**, 072507 (2006).
[12]Y. Z. Chen, J. R. Sun, S. Liang, W. M. Lv, B. G. Shen, and W. B. Wu, J. Appl. Phys. **103**, 096105 (2008).
[13]Y. Z. Chen, J. R. Sun, J. L. Zhao, J. Wang, B. G. Shen, and N. Pryds, J. Phys.: Condens. Matter **21**, 442001 (2009).
[14]Y. H. Ding, Y. Q. Wang, R. S. Cai, Y. Z. Chen, and J. R. Sun, Appl. Phys. Lett. **99**, 191914 (2011).
[15]Y. H. Ding, Y. Q. Wang, R. S. Cai, Y. Z. Chen, and J. R. Sun, Chin. Phys. B **21**, 087502 (2012).
[16]C. Y. Li, Y. Q. Wang, R. S. Cai, Y. Z. Chen, and J. R. Sun, Mater. Lett. **95**, 70 (2013).
[17]Y. Tokunaga, T. J. Sato, M. Uchida, R. Kumai, Y. Matsui, T. Arima, and Y. Tokura, Phys. Rev. B **77**, 064428 (2008).
[18]V. N. Smolyaninova, A. Biswas, C. Hill, B. G. Kim, S. W. Cheong, and R. L. Greene, J. Magn. Magn. Mater. **267**, 300 (2003).
[19]A. Kumar and J. Dho, J. Appl. Phys. **110**, 093901 (2011).
[20]G. Aurelio, D. Niebieskikwiat, R. D. Sanchez, J. Campo, G. J. Cuello, and J. Rivas, Phys. Rev. B **72**, 134405 (2005).
[21]V. Agarwal, M. P. Singh, P. K. Siwach, P. Fournier, and H. K. Singh, Phys. Status Solidi A **207**, 1922 (2010).
[22]K. Takubo, J. Y. Son, T. Mizokawa, N. Takubo, and K. Miyano, Phys. Rev. B **75**, 052408 (2007).
[23]Y. Tomioka and Y. Tokura, Phys. Rev. B **66**, 104416 (2002).
[24]Y. Y. Zhao, F. X. Hu, J. Wang, L. Chen, W. W. Gao, J. Shen, J. R. Sun, and B. G. Shen, J. Appl. Phys. **111**, 07d721 (2012).
[25]E. R. Buzin, W. Prellier, B. Mercey, C. Simon, and B. Raveau, J. Phys.: Condens. Matter **14**, 3951 (2002).
[26]X. J. Chen, Phys. Rev. B **65**, 174402 (2002).